Estimation of light-use efficiency through a combinational use of the photochemical reflectance index and vapor pressure deficit in an evergreen tropical rainforest at Pasoh, Peninsular Malaysia

Tatsuro Nakaji [1*], Yoshiko Kosugi [2], Satoru Takanashi [3], Kaoru Niiyama[3], Shoji Noguchi [3], Makoto Tani [2], Hiroyuki Oguma [4], Abdul Rahim Nik [5] and Abdul Rahman Kassim [6]

[1] Affiliation: Tomakomai Experimental Forest, Hokkaido University

Address: Takaoka, Tomakomai, Hokkaido, 053-0035 Japan

Phone/Fax.: +81-144-33-2171/+81-33-2173

E-mail: nakaji@fsc.hokudai.ac.jp

* Corresponding author

[2] Affiliation: Graduate School of Agriculture, Kyoto University

Address: Kyoto, 606-8502, Japan

E-mail: ykosugi@kais.kyoto-u.ac.jp (Y. Kosugi), tani@kais.kyoto-u.ac.jp (M. Tani)

[3] Affiliation: Forestry and Forest Products Research Institute

Address: 1 Matsunosato, Tsukuba, Ibaraki, 305-8687 Japan

E-mail: tnsatoru@ffpri.affrc.go.jp (S. Takanashi), niiya@ffpri.affrc.go.jp (K. Niiyama),

noguchi@affrc.go.jp (S. Noguchi)

[4] Affiliation: National Institute for Environmental Studies

Address: 16-2 Onogawa, Tsukuba, Ibaraki, 305-8506 Japan

E-mail: oguma@nies.go.jp

[5] Affiliation: Ministry of Natural Resources and Environment

Address: 62574 Putrajaya, Malaysia

E-mail: abdrahim.nik@gmail.com

[6] Affiliation: Forest Research Institute Malaysia

Address: 52109 Kepong, Selangor, Malaysia

E-mail: rahmank@frim.gov.my

Keywords: lowland dipterocarp forest, phenology, productivity, remote sensing, vegetation index, water conditions

Abbreviations

APAR, absorbed photosynthetically active radiation; CCI, canopy chlorophyll index; EVI, enhanced vegetation index; FWHM, full width of half maximum; GPP, gross primary

41 production; LUE, light use efficiency; NDVI, normalized difference vegetation index; PAR,
42 photosynthetically active radiation; PRI, photochemical reflectance index; SWC, volumetric soil
43 water content; T_{air}, air temperature; VI, vegetation index; VPD, vapor pressure deficit; WI,
44 water index.
45
46 **Abstract**
47
48 In the search for a better method of estimating the light-use efficiency (LUE) of evergreen
49 tropical rainforests, we employed remotely sensed spectral vegetation indices (VIs) to monitor
50 both CO_2 flux and canopy spectral reflectance over 3 years in a lowland dipterocarp forest in
51 Peninsular Malaysia. We investigated the sensitivity of five VIs calculated from spectral
52 reflectance: the photochemical reflectance index (PRI), the canopy chlorophyll index (CCI), the
53 normalized difference vegetation index (NDVI), the enhanced vegetation index (EVI) and the
54 water index (WI).

55 During the monitoring period, clear seasonal variations were not found in LUE, the
56 observed VIs or the phenological timing (particularly new leaf flush) of dominant dipterocarp
57 trees. Although leaf phenology tended to correlate with variations in the CCI, the highest
58 correlation coefficient among the relationships between LUE and the VIs was observed in PRI
59 (R = 0.341, n = 699). Among the relationships between LUE and meteorological factors, the
60 strongest correlation was found between LUE and vapor pressure deficit (VPD; R = –0.580).

These results suggest that unseasonal variation in LUE would be more affected by water conditions than leaf phenology or green leaf mass, and that the PRI has lower sensitivity for direct estimation of LUE compared to VPD in this evergreen tropical rainforest.

To improve the accuracy in estimating LUE, we examined the potential of combinational use of VIs and meteorological factors. Variable selection by stepwise multiple regression showed that the best variable combination for LUE estimation was the PRI and VPD (R = 0.612). The relative root mean square error (rRMSE) in the simple regression models using PRI, VPD and PRI×VPD, and the multiple regression model using PRI and VPD, were 22.5%, 19.4%, 19.0% and 18.7%, respectively. Based on these results, we concluded that (1) the estimation method solely based on the PRI as in the case of other temperate deciduous forests is not suitable in the tropical evergreen rainforest, and (2) the combinational use of the PRI and VPD offers one of the better models for estimating LUE in tropical evergreen rainforests.

1. Introduction

The light-use efficiency (LUE) of vegetation cover, generally expressed as the ratio of gross primary production (GPP) to absorbed photosynthetically active radiation (APAR), is one of the most essential parameters in production estimation models for terrestrial ecosystems (Monteith, 1972, 1977; Running et al., 2000; Heinsch et al., 2003; King et al., 2011). LUE is also often referred to as light conversion efficiency (ε) or radiation-use efficiency (RUE). The observed

81 value of LUE in forest ecosystems has generally ranged from 0.01 to 0.04 mol mol^{-1} (Nichol et
82 al., 2000, 2002; Strachan et al., 2002; Jenkins et al., 2007; Nakaji et al., 2007; Goerner et al.,
83 2009). Historically, spatial variations in LUE have been estimated using an empirical value for
84 each vegetation type or environmental factor function (e.g. Potter et al., 1993; Ruimy et al.,
85 1994). For example, in the MODIS GPP algorithm, one of the most commonly employed model
86 approaches for global GPP estimation, seasonal variation in LUE is estimated as the product of
87 maximum LUE (LUE_{max}) and two attenuation scalars that evaluate the responses of
88 photosynthesis to vapor pressure deficit (VPD) and air temperature (T_{air}; Heinsch et al., 2003).
89 The scalars range from 0 to 1.0, and are calculated using simple linear ramp functions of daily
90 minimum T_{air} and VPD. Although the relationships between the scalars and the input parameters
91 (e.g. VPD and minimum T_{air}) have been broadly defined in lookup tables for each biome, this
92 algorithm does not include the vegetational parameter related to the response of photosynthesis
93 to the varying environmental condition in the field. Therefore, the development of other
94 methods to estimate the *in situ* response of LUE to field conditions is emerging as an important
95 approach for monitoring the productivity response of diversified forests on a global scale.
96 From this point of view, several studies have attempted the remote estimation of variation in
97 LUE in the field, employing optical remote sensing techniques such as calculating spectral
98 vegetation indices (VIs) using spectral reflectance measurements made from above the canopy
99 (including space; Nichol et al., 2002; Drolet et al., 2005, 2008; Garbulsky et al., 2008, 2011;
100 Nakaji et al., 2008; Hall e al., 2008; Hilker et al., 2011). One of the most promising VIs used in

101 estimating LUE is the photochemical reflectance index (PRI; Gamon et al., 1992; Peñuelas et al.,
102 1995), which is generally calculated from spectral reflectance at 531 nm (the absorption band of
103 xanthophyll) and 570 nm. The PRI of green leaves shows diurnal variation due to
104 light-dependent changes in the chemical composition of xanthophylls, which play a role in
105 photoprotection (Peñuelas et al., 1994; Gamon and Surfus, 1999; Nakaji et al., 2006). In terms
106 of the timescale of seasonal variation, PRI is affected by the balance of foliar pigments such as
107 chlorophyll and carotenoids (Peñuelas et al., 1994; Sims and Gamon, 2002; Filella et al., 2004,
108 2009; Nakaji et al., 2006). Since these variations are indirectly linked to the control and
109 maintenance of photosynthetic efficiency, the PRI has been thought to be a useful indicator of
110 LUE (e.g. Filella et al., 1996; Nichol et al., 2000, 2002; Strachan et al., 2002; Drolet et al.,
111 2005; Serrano and Peñuelas, 2005; Nakaji et al., 2006; Sims et al., 2006; Cheng et al., 2009).
112 Furthermore, recently a number of studies have noted the utility of PRI for detecting changes in
113 LUE in response to drought (Suárez et al., 2008, 2009; Goerner et al., 2009;
114 Hermández-Clemente et al., 2011; Moreno et al., 2012; Zarco-Tejada et al., 2012). In addition,
115 since studies on the utility of satellite-derived PRI have also been started by some researchers
116 (Rahman et al., 2004; Drolet et al., 2005, 2008; Garbulsky et al., 2008; Hilker et al., 2011;
117 Moreno et al., 2012), understanding the effectiveness and uncertainty of this index in several
118 forest types will be important for the development of a satellite-based monitoring algorithm of
119 LUE in near future.

120 Foliar chlorophyll concentration and green leaf mass are also related to variation in LUE in

121 the field. In the case of crop field studies, large seasonal variations in LUE have been estimated
122 based on remotely sensed chlorophyll concentrations (Wu et al., 2009; Houborg et al., 2011),
123 while in the study of a temperate coniferous forest, the canopy chlorophyll index (CCI),
124 calculated from the derivative spectral reflectance around the red-edge position (Sims et al.,
125 2006), showed a significant positive relationship with LUE (Nakaji et al., 2008). Although few
126 studies have examined the relationship between LUE and the greenness-related VIs such as the
127 normalized difference vegetation index (NDVI) and the enhanced vegetation index (EVI; e.g.
128 Asrar et al., 1989; Gamon et al., 1995; Liu and Huete, 1995; Huete et al., 2002), these VIs
129 sometimes show significant correlations with LUE when the variation in LUE is governed by
130 green leaf mass (Sims et al., 2006; Nakaji et al., 2007; Mänd et al., 2010; Garbulsky et al., 2011;
131 Peñuelas et al., 2011).

132 Although several studies have been done on optical remote sensing of LUE in evergreen
133 forests, these studies have been conducted mainly in temperate coniferous forests (Nakaji et al.,
134 2008; Cheng et al., 2009; Hilker et al., 2010; Hermández-Clemente et al., 2011) and
135 Mediterranean forests (Serrano and Peñuelas, 2005; Garbulsky et al., 2008; Suárez et al., 2008;
136 Goerner et al., 2009; Moreno et al., 2012), and information concerning tropical forests is very
137 limited. In particular, our knowledge of the PRI sensitivity in tropical forests is limited to only
138 one study in Botswana (Grace et al., 2007). Therefore, understanding the utility of VIs for LUE
139 estimation in evergreen tropical forests is critical to the future discussion of remote sensing of
140 GPP on a global scale. In this study, we attempt to estimate the LUE of an evergreen tropical

141 rainforest using VIs.

142 Our research forest is a lowland dipterocarp forest in Peninsular Malaysia. In this forest,
143 there would typically be less seasonality in productivity than in other deciduous forests, as there
144 is no clearly defined dry/rainy season cycle, and little seasonal variation in the canopy leaf
145 biomass (as measured by the leaf area index, LAI). Furthermore, a previous study by Kosugi et
146 al. (2008) reported that GPP in this tropical rainforest is positively related to water status factors
147 such as soil water content (SWC). Therefore, we predicted that the sensitivity of chlorophyll-
148 and green leaf mass-related VIs (i.e. CCI, NDVI and EVI) to LUE would be relatively low
149 compared to the stress-related index, PRI. Furthermore, if these VIs alone were not adequate to
150 evaluate the variation in LUE, we expected that the combinational use of VIs and
151 meteorological factors such as T_{air}, VPD and SWC could improve the accuracy in estimating
152 LUE. In this study, we also tested the potential of water index (WI; Peñuelas et al., 1993, 1997)
153 as a supplemental variable because the water status may affect LUE. The WI reflects the
154 variation in the reflectance of water absorption band at 970 nm, and it can be an indicator of the
155 water condition of the vegetation surface (Peñuelas et al., 1993, 1997; Claudio et al., 2006;
156 Harris et al., 2006). Although the WI cannot detect the variation in LUE directly, if LUE will be
157 reduced by severe drought, additional use of WI may be useful for LUE estimation. In addition,
158 in the test of combinational use of VIs and meteorological factors, we tested the potential of the
159 PRI as substitute index evaluating attenuation scalars in a linear ramp function model.

160 Therefore, in this study, we first investigated the correlations between LUE and VIs and

meteorological parameters, and then analysed the effect of the combinational use of VIs and meteorological parameters on the accuracy of LUE estimation in an evergreen tropical rainforest.

2. Materials and methods

2.1. Study site

We observed the CO_2 flux and canopy spectral reflectance of the lowland dipterocarp forest at the Forest Research Institute Malaysia's (FRIM) Pasoh Forest Reserve (2˚58' N, 102˚18' E) in Peninsular Malaysia. This research site is one of the monitoring sites in the AsiaFlux network (for more information about the monitoring sites visit AsiaFlux's website at http://www.asiaflux.net). The elevation and area of the site are 75–150 m a.s.l. and 2450 ha, respectively. All measurements of atmosphere, canopy phenology and canopy reflectance were taken using instruments mounted on a 53-m flux-monitoring tower. The volumetric soil water content (SWC) was measured using nine sensors in three points located <20 m away from the monitoring tower, each at three different depths including 0.1, 0.2 and 0.3 m (Kosugi et al., 2012). At this research site, Kosugi et al. (2007) investigated the spatio-temporal variation of SWC in a 50 m × 50-m plot around the flux-monitoring tower for 3 years. They had previously reported that the large spatial variation of SWC within the plot ranged from 15% to 31% of the

coefficient of variation (Kosugi et al., 2007). As for the seasonal trends, continuously observed SWC near the tower was correlated significantly with widely measured SWC in the 50 m × 50-m plot ($P < 0.01$; after Kosugi et al., 2007). Therefore, in this study, we used the SWC measured at the tower as one of the environmental factors explaining the variation in LUE.

In this study, we analysed field data obtained between 15 October 2008 and 31 December 2011. Mean air temperature during the monitoring period ranged from 24.8˚C to 25.3˚C, which was similar to the mean annual air temperature observed over the 9 years from 2003 to 2011 (25.3˚C). However, the annual precipitation in 2009 was 25% lower than the average for those 9 years, and both a reduction in SWC and an increase in atmospheric VPD, of 6% and 7% respectively, occurred compared to the 9-year average (Kosugi et al., 2012). Thus, 2009 was considered a dry year in the Pasoh Forest Reserve.

The total number of plant species in the forest reserve was over 800 (Kochummen, 1997). The dominant canopy tree species around the monitoring tower were *Dipterocarpus sublamellatus*, *Neobalanocarpus heimii*, *Xanthophyllum stipitatum* and *Ptychopyxis caput-medusae*. The continuous canopy height was about 35 m, and some emergent trees exceeded 45 m. Leaf biomass at the research site was relatively high with an LAI of 6.52 (Kosugi et al., 2008).

2.2. Canopy spectral reflectance and spectral vegetation indices

201 The hyperspectral reflectance of the forest canopy was monitored using two tower-mounted
202 spectroradiometers (MS-700, Eko Instruments Co. Ltd., Tokyo, Japan). The full width at half
203 maximum (FWHM) and sampling interval of the spectroradiometers were 10 nm and 3.3 nm,
204 respectively. One spectroradiometer was mounted on the tower top (53 m) to monitor solar
205 radiation (i.e. spectral irradiance), and the other was affixed to the lower side of a horizontal
206 boom that extended 3 m from the 53-m-tall tower, at a height of 50 m, to measure solar energy
207 reflected from tree canopies (i.e. reflected spectral radiance). The radiometers were powered by
208 solar-generated electricity. The field of view (FOV) of this sensor is 180°, and the vertical
209 distance between the sensor and forest canopy was about 15 m. According to tree census data
210 (Niiyama et al., unpublished data), the tree density (DBH > 5 cm) and number of tree species
211 around the tower are 11.6 individual/100 m^2 and 7.5 species/100 m^2, respectively. These values
212 suggest that 82 individual trees of 53 species grow in the area of half angle of FOV (i.e. 30 m
213 diameter circle). About 30 tall trees were observed on the canopy surface of this area.
214 Spectral irradiance and spectral reflected radiance (from 400 nm to 1050 nm) were
215 measured at 5-min intervals during the daytime (Fig. 1a). There was a difference in sensitivity
216 of less than 5% between two spectroradiometers. To correct this effect on the sensor-derived
217 reflectance, we calculated the signal ratio between the two spectroradiometers in each waveband
218 by measuring the diurnal variation in solar radiation under clear sky conditions at a half-year
219 interval. The canopy spectral reflectance was derived by dividing reflected spectral radiance,
220 corrected for the difference in instrument sensitivity, by spectral irradiance (Fig. 1b).

221 Using the canopy spectral reflectance, we calculated five VIs as shown in Table 1. Two
222 green leaf mass-related VIs, NDVI (Tucker, 1979) and EVI (Huete et al., 2002), were calculated
223 from measurements of the broadband reflectances in the visible and near-infrared spectral
224 regions. We calculated these broadband reflectances from the MS-700 original bands after
225 averaging seven bands on both sides of the target wavelength. The PRI (Gamon et al., 1992,
226 1997; Peñuelas et al. 1995) and the CCI (Sims et al., 2006) were calculated with the reflectance
227 values in two or four narrow wavebands located in the visible region of the spectrum. These
228 narrow wavebands were derived from three bands averaged value around the target wavelength.
229 The WI (Peñuelas et al., 1993, 1997) was calculated from broadband reflectances at 900 nm and
230 970 nm after binning treatment. Each VI was calculated for each 5-min interval and was
231 averaged for each half hour.
232
233 *2.3. Leaf phenology*
234
235 To record the phenological features of the dipterocarp trees, a canopy photograph was taken
236 at daily intervals using a digital camera set near the downward-looking spectroradiometer. The
237 monitoring camera was fixed at the 50-m point of the monitoring tower and captured the four
238 large tree canopies under the spectroradiometer. We used a 1.3 M pixel field monitoring camera
239 (KADEC21-EYE II, North One Co. Ltd., Sapporo, Japan) from September 2009 to January
240 2011, and a 5 M pixel camera with a photovoltaic battery system (Timelapse PlantCam,

241 Wingscapes Inc., Alabaster, AL, USA) from February 2011 to December 2011. The timings and
242 degree of new leaf flush, leaf growth (expansion) and defoliation were discriminated by eye
243 using colour photo images. We principally analysed two *D. sublamellatus* trees near the
244 monitoring tower (Fig. 2a). The leaf emergence (leaf flush) of *D. sublamellatus* was observed
245 together with defoliation (Fig. 2b), but the defoliation was complete before the full expansion of
246 new leaves (Fig. 2c). The leaf expansion and new leaf emergence continued over 3 months (Fig.
247 2d). We recorded the timing of initiation of new leaf flush and compared the timing to the time
248 course of the VIs.
249
250 *2.4. CO_2 flux and light-use efficiency*
251
252 We estimated GPP from CO_2 flux measurements and measured PAR above the canopy
253 surface to calculate LUE in the lowland dipterocarp forest. GPP was estimated from canopy
254 CO_2 flux (*Fc*), variations in CO_2 storage (*Sc*) and daytime ecosystem respiration (RE), as
255 follows:
256
257 $$GPP = -(Fc + Sc) + RE. \quad (1)$$
258
259 *Fc* was measured with tower-mounted instruments at a height of 54 m using the eddy
260 covariance method, and *Sc* was estimated from the time course of changes in CO_2 concentration

261 at 10 heights (Ohkubo et al., 2008). The negative value of *Fc* indicates CO_2 uptake by
262 vegetation. In an ecosystem with a tall canopy such as a tropical forest, it is necessary to
263 consider the storage of CO_2 under the canopy for exact estimation of GPP (Baldocchi et al.,
264 2001). *Sc* primarily indicates the mass change in CO_2 gas under the canopy, and its effects can
265 be corrected by calculating the sum of *Fc* and *Sc*. Daytime ecosystem respiration was estimated
266 from the relationship between soil water content and nocturnal CO_2 flux (Kosugi et al., 2012).
267 The concentrations of CO_2 and H_2O were monitored with an open-path infrared gas analyzer
268 (IRGA; LI-7500 or LI-7500A, Li-Cor, Inc., Lincoln, NE, USA), and the wind speed and
269 temperature were measured with a three-axis sonic anemometer (SAT-550, Kaijo, Tokyo, Japan).
270 The methods used for the calculation of *Fc* and *Fs* at the Pasoh research site are detailed in
271 Kosugi et al. (2012). All of the measured parameters were used to calculate GPP every half
272 hour.

273 We calculated LUE as the ratio of GPP to APAR.

274

275 $$LUE = GPP/APAR. \quad (2)$$

276 $$APAR = FAPAR*PAR. \quad (3)$$

277 $$FAPAR = (PAR – PARr – PARt + PARs)/PAR, \quad (4)$$

278

279 where FAPAR is a fraction of APAR ranging from 0 to 1.0, PARr is the PAR reflected from the
280 canopy surface, PARt is the PAR transmitted through the canopy and PARs is the PAR reflected

281 from the ground surface. All PAR values were measured using downward or upward PAR
282 sensors (LI-190, Li-Cor) mounted on the tower. In this paper, we used only original GPP data in
283 our analysis; thus, for example, supplemental GPP data created using a gap filling method
284 involving a light response curve or lookup table was not used. Only those half-hourly values for
285 the VIs, GPP and LUE, calculated from measurements taken under clear skies from 12:00 to
286 14:00, were used for correlation analysis. The threshold for determining "clear sky conditions"
287 was a relative irradiance of 75% of full sunlight (Nakaji et al., 2007). Because the mean
288 culmination time in this site is 13:11, we used the average data around 13:00. As shown in Fig. 3,
289 the effect of solar angle on VIs was relatively small in this time period. The total dataset
290 resulted in 699 (days).
291
292 *2.5. Statistical analysis*
293
294 Pearson's correlation test was used to examine the significance of the relationship between
295 LUE and the VIs, and between LUE and the meteorological parameters (T_{air}, VPD and SWC).
296 Simple regression analysis and stepwise multiple regression analysis were used in developing
297 the LUE estimation models. Stepwise multiple regression was used to select the best
298 combination of variables at variance inflation factor (VIF) <2.0. The validation of the estimation
299 model was performed using the resubstitution estimation method (n = 699). All statistical
300 analyses were performed using SPSS software (11.0.1J, SPSS Inc., Tokyo, Japan).

301

302 **3. Results and discussion**

303

304 *3.1. Time courses of meteorological parameters, phenology and productivity*

305

306 As shown in Fig. 4, T_{air}, VPD and SWC in the lowland dipterocarp forest in the Pasoh Forest
307 Reserve showed representative seasonal variations, most notably in 2010 and 2011. A reduction
308 in temperature was observed near year-end, and the period from the end of the year through the
309 beginning of the next (December–February) showed the characteristics of a slight dry season,
310 with a reduction in SWC and increase in VPD in each year during this period (Fig. 4a).
311 However, unusual trends in SWC and VPD were observed in mid-2009. The total rainfall
312 during the second and third quarters (April–September) of 2009 was 41% less than the average
313 for the same period over the 9 years from 2003 to 2011 (data not shown). This shortage of
314 rainfall intermittently depressed SWC levels to 0.22 m^3 m^{-3}, and increased VPD above 10 hPa
315 in mid-2009 (Fig. 4a). In this evergreen tropical rainforest, since FAPAR had an almost constant
316 value of ~0.955 (±0.012), large variations were not observed in APAR (Fig. 4b).

317 The time courses of leaf phenology (new leaf flush), the productivity parameters (GPP and
318 LUE) and the remotely sensed VIs (NDVI, EVI, CCI and PRI) are shown in Fig. 5. With regard
319 to GPP and LUE, clear periodic variations typically observed in other biomes (e.g. Nakaji et al.,
320 2008; Moreno et al., 2012) were not detected in this dipterocarp forest, and water conditions

seemed to exert a stronger influence on these parameters than leaf phenology. Although some gaps occurred in the original CO_2 eddy flux data, detectable declining trends in GPP and LUE were observed to correspond to increases in VPD and reductions in SWC; for example, from January 2010 to March 2010, declines in GPP and LUE were observed in conjunction with increases in VPD and reductions in SWC (Figs. 4a and 5a).

New leaf flush in *D. sublamellatus*, one of the most dominant tree species around the monitoring tower, was occurred two times in 2010 and four times in 2011 (Fig. 5). In most of these instances, the leaf flush appeared across the entire canopy surface, but the leaf flush in September 2011 was observed in only part of the canopy (<30% of the surface area). Osada et al. (2012) analysed the leaf phenology of *D. sublamellatus* in Pasoh over 3 years beginning in 1995. They reported that *D. sublamellatus* showed inconsistent phenological patterning in leaf emergence, and our results support their findings.

As shown in Fig. 5a, no clear links were discovered between the timing of phenological events and trends in productivity variables. We infer two main reasons why the camera-observed phenological events did not clearly correlate with flux-based productivity in this forest. The first is that water status had a greater impact on CO_2 than leaf phenology. Water conditions in the atmosphere (VPD) and soil (SWC) are well known to affect the photosynthetic rate. For example, in the Amazonian transitional tropical forest, although the air temperature did not differ between the dry and wet seasons, a large reduction in net primary production (NPP) was observed in the dry season when the VPD exceeded 8 hPa (Vourlitis et al., 2001). A high

VPD typically lowers the photosynthetic rate indirectly by inducing stomatal closure to avoid water stress (Lloyd and Farquhar, 2008). Similarly, in the forest of the present study, the relatively high VPD of about 10 hPa would be one of the causes of a reduction in GPP. A positive relationship between SWC and GPP in this lowland dipterocarp forest has been reported by Kosugi et al. (2012). Based on the analysis of 7 years of monitoring data from 2003 to 2009, they found that soil dryness reduced ecosystem respiration (RE) and GPP (Kosugi et al., 2012). In the present forest, because the variation in APAR is relatively small (Fig. 3b), VPD and SWC would be strong determining factors both of GPP and LUE. Furthermore, the new leaf flush of *D. sublamellatus* and of many other dipterocarp species in Pasoh typically occurred together with defoliation, and change in leaf mass during this event was relatively small (Osada et al., 2003, 2012). This finding suggests that the effects of phenological events on productivity are limited.

The second reason alluded to the above is the limited representativeness of camera data, given the considerable diversity of tree species in this tropical forest. Leaf phenology in this forest has been reported to be roughly synchronised among the major dipterocarp species (Osada et al., 2003). However, the contribution of camera-derived phenology data for a single dominant species near the tower would be limited in evaluating seasonal trends in CO_2 flux because the eddy flux reflects the overall ecophysiological condition of many tree species within its large footprint. A tower-mounted camera is a useful tool for ecological studies in forests (e.g. Richardson et al., 2007; Ide and Oguma, 2010), but the limitations of

361 camera-derived phenology data have been noted in the case of deciduous forests (Hufkens et al.,
362 2012). In the case of tropical forests showing similarly high diversity, improvements in the
363 method of monitoring tree phenology, such as the additional or combinational use of satellite
364 remote sensing data, should be considered in future studies.
365
366 *3.2. Time course of remotely sensed VIs*
367
368 The classic greenness-related VIs, such as the NDVI and the EVI, showed rather small
369 variations of less than 0.1 (Fig. 5b). Comparing the VIs and leaf phenology, the timing of new
370 leaf flush was not closely matched by troughs or peaks in these broadband VIs (Fig. 5b). The
371 NDVI and the EVI are commonly used as phenology indicators for deciduous forests, where
372 leaf expansion in the spring can be detected as an increase in the VIs (e.g. White et al., 1997;
373 Ganguly et al., 2010; Liang et al., 2011; Nakaji et al., 2011; Soudani et al., 2012). However, in
374 the evergreen forest, while the suitability of the NDVI as a spring phenology index has been
375 tested in a boreal coniferous forest, it has been reported that the direct detection of spring bud
376 break was difficult by using the NDVI because the variation in leaf mass change was small and
377 gradual (Jönsson et al., 2010). Furthermore, it is well known that the sensitivity of the NDVI to
378 variations in LAI is saturated in dense canopies (LAI > 2~6) (Gamon et al., 1995; Huemmrich et
379 al., 1999: Viña et al., 2011). Therefore, in this study, low sensitivities of the NDVI and the EVI
380 would be caused by small seasonal variation in LAI (≈FAPAR) (Fig. 4b) and high LAI (6.52)

(Kosugi et al., 2008). These results suggest that the protocol used in the estimation of phenological events in deciduous forests is less accurate in the case of an evergreen tropical rainforest.

Relatively large time-course variations were observed in the CCI and the PRI. During the overlapping monitoring period of canopy photographs and spectral reflectance, most of the troughs in the CCI were coincident with new leaf flushes, except in September 2010 and April 2011 (Fig. 5c). Since the CCI is based on variations in the derivative spectrum around the red edge (Sims et al., 2006), small variations in chlorophyll concentration resulting from the appearance of new leaves can be detected with greater sensitivity than in the case of the greenness-related VIs. The red-edge-based indices obtained from satellite data (such as the MERIS chlorophyll index) have been reported to be good indicators of vegetation phenology and productivity (Dash et al., 2010; Harris and Dash, 2010; Viña et al., 2011). Thus, in addition to its proven capacity to detect new leaf flush in a deciduous forest (as an increase in the CCI value), our results suggest that even in a tropical evergreen dipterocarp forest, the CCI should provide a sensitive indicator of canopy conditions regardless of the relationship between phenology and productivity.

The time course of PRI was roughly similar to that of the CCI, and several clear declines in the PRI were coincident with those in the CCI (e.g. February 2009, April 2009, October 2009, July 2010 and July 2011; Fig. 5c). The PRI can track not only short-term variations in foliar xanthophylls in response to irradiation, but also long-term variations in the balance of

401 carotenoids and chlorophylls (Gamon et al., 1992; Peñuelas et al., 1994; Sims and Gamon,
402 2002; Filella et al., 2004, 2009; Nakaji et al., 2006; Rahimzadeh-Bajgiran et al., 2012). The
403 reductions in the PRI corresponding to the CCI suggest that the appearance of new leaves,
404 which have low chlorophyll concentrations, reduced the PRI. However, many small troughs in
405 the PRI (e.g. in May 2009, December 2009 and March 2010) were not reflected in the CCI (Fig.
406 5c), but these small troughs were coincident with peaks in VPD and reduction in LUE (Fig. 5a).
407 Studies have reported that the photosynthetic response to drought stress can be detected by the
408 PRI in Mediterranean shrubs and conifers (Peñuelas et al., 1997; Filella et al., 2004; Suárez et
409 al., 2008, 2009; Goerner et al., 2009; Hermández-Clemente et al., 2011; Moreno et al., 2012).
410 Although we have not measured the degree of photoinhibition and stomatal responses of canopy
411 leaves directly, the time courses of the PRI, LUE and VPD suggest the potential of PRI for
412 detecting the photosynthetic response of tropical evergreen trees to varying water status.
413 The WI is one of the most useful indices for estimating the degree of dryness of plant tissue
414 (Peñuelas et al., 1993, 1997). In this forest, however, the WI did not show clear seasonal
415 variations or small troughs as shown by VPD (Fig. 5b). The range of variation of WI was only
416 0.04 during the observation period (0.94–0.98; Fig. 5b). Based on the report on the relationship
417 between the WI and leaf water content in Mediterranean evergreen plants (Peñuelas et al., 1997),
418 this range of WI corresponds to 80–100% of dry mass-basis plant water content, which
419 generally does not cause wilting in tree leaves. Therefore, we speculate that the air dryness
420 and/or soil dryness would depress the photosynthetic activity (i.e. LUE) without severe

421 desiccation of leaves or a large variation in green leaf mass in this forest. Overall, although leaf
422 phenology was detectable by the CCI and the PRI, small variations of LUE in this evergreen
423 tropical rainforest would be related to VPD and the PRI.
424
425 *3.3. Estimation of LUE using the VIs and meteorological parameters*
426
427 Table 2 shows the results of the single and multiple regression analysis. All the VIs and
428 meteorological parameters showed significant relationships with LUE. In terms of the
429 relationship between the VIs and LUE, although a positive correlation between the CCI and
430 LUE was detected, the strongest correlation was found between the PRI and LUE. This result
431 supports our prediction that the PRI is one of the best remotely sensed indices for monitoring
432 LUE, even in evergreen tropical rainforests. Since the PRI has a high sensitivity to both
433 pigmentation status and stress response, it can detect small variations in LUE better than the
434 CCI and other greenness-related VIs. However, the coefficient of determination (R^2) in the
435 PRI-based regression model was only 0.116 in this case, a lower value than for other forests
436 such as broadleaf, conifer and tundra (0.5–0.7 of median R^2; Garbulsky et al., 2011).
437 Furthermore, our results indicate that the PRI–LUE regression function would show site
438 differences. For example, the slope value of 0.256 for this evergreen tropical forest (Table 2) is
439 higher than the 0.126 reported for a cool–temperate young coniferous forest and the 0.202 for a
440 temperate evergreen coniferous forest (Nakaji et al., 2008). Although the reported LUEs have

been calculated as GPP/PAR, lower slope values from 0.081 to 0.185 have been observed for boreal forests by Nichol et al. (2000, 2002). According to the studies by Hall et al. (2008), the slope of PRI–LUE regression line is reduced with increasing shaded leaves because non light-saturated leaves sometimes had higher LUE without great reduction in PRI compared to sunlit leaves. Therefore, Hilker et al. (2011) demonstrated that the shading factor calculated from canopy structure can improve PRI-based LUE estimation accuracy over several forests. In this study, although we have not deal with structure differences and shadow factor, lower slope of PRI–LUE regression function in sparse boreal stand (Nichol et al., 2002) rather than that in dense tropical evergreen forest (this study) suggest that the effect of shading would be one of the causes of site-dependent differences. Grace et al. (2007) and Garbulsky et al. (2011) have noted the differing sensitivity of the PRI in the case of different vegetation types. Our findings similarly indicate that in the case of evergreen tropical rainforests, we should be aware of the significant uncertainty involved in the use of an empirical simple regression model based on PRI, and several site-dependent adjustments of coefficients are necessary when global estimation of LUE is conducted using PRI. With considering the combinational use of structural parameter (i.e. shading factor), the development of a standardised PRI index that buffers all the associated factors driving its change in addition to LUE itself is also desired.

In terms of the relationships between LUE and meteorological parameters, a higher R^2 than for the PRI-based model was found between LUE and VPD (R^2 = 0.336), and between LUE and T_{air} (R^2 = 0.201; Table 2). The negative slope of the regression function between LUE and these

variables indicate that air dryness and heat stress may depress the photosynthetic rate in this tropical rainforest. However, of all the combinations in the stepwise multiple regression analysis, the best variable combination for LUE estimation was that of PRI and VPD (Table 2). Neither T_{air}, SWC nor WI were selected as significant variables, even when the number of variables was increased to three (in this case, EVI was selected). The mechanism of variance in LUE cannot be fully elucidated using only stepwise multiple regression analysis, but these selected variables suggest that water status, pigment balance and photoinhibition would affect the photosynthesis of this forest in a complex manner.

The R^2 value was highest in the multiple regression model using PRI and VPD among all test cases (0.375; Table 2). We also tested a simple regression model using the product of PRI*VPD, and the R^2 of this model was 0.352, an intermediate value between the single regression model using VPD and the multiple regression model using PRI and VPD (Table 2). In addition, if LUE_{max} in this forest were defined as the maximum value of weekly mean LUE (0.022 mol mol^{-1}), the regression model using PRI*VPD could be expressed as a simple function {$LUE = LUE_{max}*[1.02 + 0.79*(PRI*VPD)]$; Table 2}. Although the form of the function is different from the linear ramp regression of attenuation scalars, this empirical function may conceivably provide a basis for the development of an alternative LUE estimation model using PRI.

Finally, Fig. 6 shows the validation of the regression models that yielded the highest R^2 in each regression group. Although the explanatory capability of the variance in LUE was less than

481 38% in all cases (i.e. $R^2 < 0.38$), the estimation error (relative root mean square error, *r*RMSE)
482 was improved by 3.6% in the combinational use of VPD and PRI compared to the use of PRI
483 alone. We found that the estimated LUE was limited to a range of 0.011–0.017 mol mol^{-1} when
484 using a model with the PRI alone, but the addition of VPD to the model expanded the range to
485 0.010–0.022 mol mol^{-1}.
486
487 **4. Conclusions**
488
489 This study resulted in two main findings concerning the utility of remotely sensed VIs for
490 the estimation of LUE in an evergreen tropical rainforest showing small variations in LUE and
491 green leaf mass. First, we showed the limited sensitivity of the PRI and the advantage of
492 meteorological factors such as VPD in a simple regression model. The explanatory capability of
493 the PRI regarding daily variation in LUE is significantly less than that of meteorological
494 parameters such as VPD and T_{air}, although the PRI is a more effective remotely sensed VI than
495 greenness- or chlorophyll-related VIs. The comparison of slope of the PRI–LUE regression line
496 among different forests indicated that the PRI sensitivity might change with varying latitude (i.e.
497 high slope in lower latitudes). If this gradational variation is true, we should also consider this
498 variation for global use of the PRI. Second, we proposed the combinational use of VPD and PRI
499 to improve the accuracy in estimating LUE. Although the prediction ability of the proposed
500 empirical model (e.g. $R^2 = 0.375$) was not higher than the regression models for other vegetation

types using PRI (R^2 = 0.38–0.60; Garbulsky et al., 2011), supplemental use of PRI would be one of the effective methods for remote sensing of LUE in evergreen forests.

Acknowledgements

This work was supported by a JSPS Grant-in-Aid for Scientific Research (KAKENHI: 20255010, 24255014) and the joint research project between the Forest Research Institute Malaysia (FRIM), the Universiti Putra Malaysia (UPM) and the National Institute of Environmental Studies (NIES). We are greatly indebted to Prof. M. Tani (Kyoto University), Dr. R. Ide (NIES), Dr. S. Ohkubo (National Agriculture and Food Research Organisation) and the staff of the Pasoh Field Research Station both for their technical support in the field monitoring and for valuable discussion.

References

Asrar, G., Myneni, R.B., & Kanemasu, E.T. (1989). Estimation of plant canopy attributes from spectral reflectance measurements. In G. Asrar (Ed.), Theory and applications of optical remote sensing (pp. 252−297). New York: John Wiley and Sons.

Baldocchi D., Falge E., Gu L., Olson R., Hollinger D., Running S., Anthoni P., Bernhofer Ch., Davis K., Evans R., Fuentes J., Goldstein A., Katul G., Law B., Lee X., Malhi Y., Meyers

521 T., Munger W., Oechel W., Paw K. T., Pilegaard K., Schmid H. P., Valentini R., Verma S.,
522 Vesala T., Wilson K. and Wofsy S. (2001) FLUXNET: a new tool to study the temporal
523 and spatial variability of ecosystem-scale carbon dioxide, water vapor, and energy flux
524 densities, *Bulletin of the American Meteorological Society*, 82:2415-2434.
525 Cheng, Y-B., Middleton, E.M., Hilker, T., Coops, N.C., Black, T.A., & Krishnan, P., (2009).
526 Dynamics of spectral bio-indicators and their correlations with light use efficiency using
527 directional observations at a Douglas-fir forest. *Measurement Science and Technology*, 20,
528 doi:10.1088/0957-0233/20/9/095107.
529 Claudio, H.C., Cheng, Y., Fuentes, D.A., Gamon, J.A., Luo, H., Oechel, W., Qiu, H.-L., Rahman,
530 A.F., & Sims, D.A. (2006). Monitoring drought effects on vegetation water content and
531 fluxes in chaparral with the 970 nm water band index. Remote Sensing of Environment,
532 103, 304–311.
533 Dash, J., Jeganathan, C., & Atkinson, P.M. (2010). The use of MERIS Terrestrial Chlorophyll
534 Index to study spatio-temporal variation in vegetation phenology over India. *Remote*
535 *Sensing of Environment*, 114, 1388-1402.
536 Drolet G., Huemmrich, K.F., Hall, F.G., Middleton, E.M., Black, T.A., Barr, A.G., & Margolis,
537 H. A. (2005). A MODIS-derived photochemical reflectance index to detect inter-annual
538 variations in the photosynthetic light-use efficiency of a boreal deciduous forest. *Remote*
539 *Sensing of Environment*, 98, 212–224.
540 Drolet, G.G., Middleton, E.M., Huemmrich, K.F., Hall, F.G., Amiro, B.D., Barr, A.G., Black,

T.A., McCaughey, J.H., & Margolis, H.A. (2008). Regional mapping of gross light-use efficiency using MODIS spectral indices. *Remote Sensing of Environment,* 112, 3064−3078.

Filella, I,, Porcar-Castell, A., Munné-Bosch, S., Bäck, J., Garbulsky, M. F., & Peñuelas, J. (2009). PRI assessment of long-term changes in carotenoids/chlorophyll ratio and short-term changes in de-epoxidation state of the xanthophyll cycle. *International Journal of Remote Sensing*, 30, 4443-4455.

Filella, I., Amaro, T., Araus, J.L., & Peñuelas, J. (1996). Relationship between photosynthetic radiation-use efficiency of barley canopies and the photochemical reflectance index (PRI). *Physiologia Plantarum*, 96, 211–216.

Filella, I., Peñuelas, J., Llorens, L., & Estiarte, M. (2004). Reflectance assessment of seasonal and annual changes in biomass and CO2 uptake of a Mediterranean shrubland submitted to experimental warming and drought. *Remote Sensing of Environment*, 90, 308−318.

Gamon, J.A., & Surfus, J.S. (1999). Assessing leaf pigment content and activity with a reflectometer. *New Phytologist*, 143, 105-117.

Gamon, J.A., Field, C.B., Goulden, M.L., Griffin, K.L., Hartley, A.E., Joel, G., Peñuelas, J., & Valentini, R. (1995). Relationships between NDVI, canopy structure, and photosynthesis in three Californian vegetation types. *Ecological Application*, 5, 28–41.

Gamon, J.A., Peñuelas, J., & Field, C.B. (1992). A narrow-waveband spectral index that tracks diurnal changes in photosynthetic efficiency. *Remote Sensing of Environment,* 41, 35–44.

561 Ganguly, S., Friedl, M.A., Tan, B., Zhang, X., & Verma, M. (2010). Land surface phenology
562 from MODIS: Characterization of the Collection 5 global land cover dynamics product.
563 *Remote Sensing of Environment*, 114, 1805–1816.
564 Garbulsky, M. F., Peñuelas, J., Papale, D., & Filella, I. (2008b). Remote estimation of carbon
565 dioxide uptake of a Mediterranean forest. *Global Change Biology*, 14, 2860−2867.
566 Garbulsky, M.F., Peñuelas, J., Gamon, J., Inoue, Y. & Filella, I. (2011). The photochemical
567 reflectance index (PRI) and the remote sensing of leaf, canopy and ecosystem radiation use
568 efficiencies. A review and meta-analysis. *Remote Sensing of Environment*, 115, 281-297.
569 Goerner, A., Reichstein, M., & Rambal, S. (2009). Tracking seasonal drought effects on
570 ecosystem light use efficiency with satellite-based PRI in a Mediterranean forest. *Remote*
571 *Sensing of Environment*, 113, 1101–1111.
572 Grace, J., Nichol, C., Disney, M., Lewis, P., Quaife, T., & Bowyer, P. (2007). Can we measure
573 terrestrial photosynthesis from space directly, using spectral reflectance and fluorescence?
574 *Global Change Biology*, 13, 1484−1497.
575 Hall, F.G., Hilker, T., Coops, N.C., Lyapustin, A., Huemmrich, K.F., Middleton, E., Margolis,
576 H., Drolet, G., & Black, T.A. (2008). Multiangle remote sensing of forest light use
577 efficiency by observing PRI variation with canopy shadow fraction, *Remote Sensing of*
578 *Environment*,112, 3201–3211.
579 Harris, A., & Dash, J. (2010). The potential of the MERIS Terrestrial Chlorophyll Index for
580 carbon flux estimation. *Remote Sensing of Environment*, 114, 1856–1862.

581 Harris, A., Bryant, R.G., & Baird, A.J. (2006). Mapping the effects of water stress on
582 Sphagnum: Preliminary observations using airborne remote sensing. Remote Sensing of
583 Environment, 100, 363–378.
584 Heinsch, F.A., Reeves, M., Votava, P., Kang, S.Y., Milesi, C., Zhao, M.S., Glassy, J., Jolly, W.
585 M., Loehman, R., Bowker, C.F., Kimball, J.S., Nemani, R.R., & Running, S.W. (2003).
586 User's guide, GPP and NPP (MOD17A2/A3) products, NASA MODIS land algorithm,
587 version 2.0. pp. 1-57.
588 Hermández-Clemente, R., Navarro-Cerrillo, R.M., Suárez, L., Morales, F., & Zarco-Tejada, P.J.
589 (2011). Assessing structural effects on PRI for stress detection in conifer forests. *Remote*
590 *Sensing of Environment,* 115, 2360-2375.
591 Hilker, T., Hall, F.G., Coops, N.C., Lyapustin, A., Wang, Y., Nesic, Z., Grant, N., Andrew Black,
592 T., Wulder, M.A., Kljun, N., Hopkinson, C., & Chasmer, L. (2010). Remote sensing of
593 photosynthetic light-use efficiency across two forested biomes: Spatial scaling. *Remote*
594 *Sensing of Environment,* 114, 2863-2874.
595 Hilker, T., Coops, N.C., Hall, F.G., Nichol, C.J, Lyapustin, A., Black, T.A., Wulder, M.A.,
596 Leuning, R., Barr, A., Hollinger, D.Y., Munger, J.W., & Tucker, C.J. (2011). Inferring
597 terrestrial photosynthetic light use efficiency of temperate ecosystems from space. *Journal*
598 *of Geophysical Research*, Vol. 116, G03014, doi:10.1029/2011JG001692.
599 Houborg, R., Anderson, M.C., Daughtry, C.S.T., Kustas, W.P., & Rodell, M. (2011). Using leaf
600 chlorophyll to parameterize light-use-efficiency within a thermal-based carbon, water and

601 energy exchange model. *Remote Sensing of Environment*, 1694-1705.
602 Huemmrich, K.F., Black, T., Jarvis, P.G., McCaughey, J.H., & Hall, F.G. (1999). High temporal
603 resolution NDVI phenology from micrometeorological radiation sensors. *Journal of*
604 *Geophysical Research*, 104, 27935-27944.
605 Huete, A., Didan, K., Miura, T., Rodriguez, E.P., Gao, X., & Ferreira, L.G. (2002). Overview of
606 the radiometric and biophysical performance of the MODIS vegetation indices. *Remote*
607 *Sensing of Environment*, 83, 195–213.
608 Hufkens, K., Friedl, M., Sonnentag, O., Braswell, B.H., Milliman, T., & Richardson, A.D.
609 (2012). Linking near-surface and satellite remote sensing measurements of deciduous
610 broadleaf forest phenology. *Remote Sensing of Environment*, 117, 307-321.
611 Ide, R., & Oguma, H. (2010). Use of digital cameras for phenological observations, *Ecological*
612 *Informatics*, doi:10.1016/j.ecoinf.2010.07.002
613 Jenkins, J.P., Richardson, A.D., Braswell, B.H., Ollinger, S.V., Hollinger, D.Y., & Smith, M.-L.
614 (2007). Refining light-use efficiency calculations for a deciduous forest canopy using
615 simultaneous tower-based carbon flux and radiometric measurements. *Agricultural and*
616 *Forest Meteorology*, 143, 64-79.
617 Jönsson, A.M., Eklundh, L., Hellström, M., & Jönsson, P. (2010). Annual changes in MODIS
618 vegetation indices of Swedish coniferous forests in relation to snow dynamics and tree
619 phenology. *Remote Sensing of Environment*, 114, 2719-2730.
620 King, D.A., Turner, D.P., & Ritts, W.D. (2011). Parameterization of a diagnostic carbon cycle

621 model for continental scale application. *Remote Sensing of Environment,* 115, 1653-1664.
622 Kochummen, K.M. (1997). Tree flora of Pasoh forest. (pp. 462). Kuala Lumpur: Forest
623 Research Institute Malaysia.
624 Kosugi, Y., Takanashi, S., Ohkubo, S., Matsuo, N., Tani, M., Mitani, T., Tsutsumi, D., & Abdul
625 Rahim, N. (2008). CO_2 exchange of a tropical rainforest at Pasoh in Peninsular Malaysia.
626 *Agricultural and Forest Meteorology,* 148, 439-452.
627 Kosugi, Y., Takanashi, S., Tani, M., Ohkubo, S., Matsuo, N., Itoh, M., Noguchi, S., & Abdul
628 Rahim, N. (2012). Influence of inter-annual climate variability on evapotranspiration and
629 canopy CO_2 exchange of a tropical rainforest in Peninsular Malaysia. *Journal of Forest*
630 *Research,* 17, 227-240.
631 Liang, L., Schwartz, M.D., & Fei, S. (2011). Validating satellite phenology through intensive
632 ground observation and landscape scaling in a mixed seasonal forest. *Remote Sensing of*
633 *Environment,* 143-157.
634 Liu, H.Q., & Huete, A.R. (1995). A feedback based modification of the NDVI to minimize soil
635 and atmospheric noise. *IEEE Transactions on Geoscience and Remote Sensing,* 33,
636 457-465.
637 Monteith, J.L. (1972). Solar radiation and productivity in tropical ecosystems. *Journal of*
638 *Applied Ecology,* 9, 747–766.
639 Monteith, J.L. (1977). Climate and efficiency of crop production in Britain. *Philosophical*
640 *Transactions of the Royal Society of London B* 277–294.

641 Moreno, A., Maselli, F., Gilabert, M.A., Chiesi, M., Martínez, B., & Seufert, G. (2012).
642 Assessment of MODIS imagery to track light-use efficiency in a water-limited
643 Mediterranean pine forest. *Remote Sensing of Environment*, 123, 359-367.
644 Mänd, P., Hallik, L., Peñuelas, J., Nilson, T., Duce, P., Emmett, B.A., Beier, C., Estiarte, M.,
645 Garadnai, J., Kalapos, T., Schmidt, I.K., Kovács-Láng, E., Prieto, P., Tietema, A.,
646 Westerveld, J.W., & Kull, O. (2010). Responses of the reflectance indices PRI and NDVI to
647 experimental warming and drought in European shrublands along a north–south climatic
648 gradient. *Remote Sensing of Environment*, 114, 626-636.
649 Nakaji, T., Ide, R., Oguma, H., Saigusa, N., & Fujinuma, Y. (2007). Utility of spectral
650 vegetation index for estimation of gross CO_2 flux under varied sky conditions. *Remote*
651 *Sensing of Environment*, 109, 274–284.
652 Nakaji, T., Ide, R., Takagi, K., Kosugi, Y., Ohkubo, S., Nishida, K., Saigusa, N. & Oguma, H.
653 (2008). Utility of spectral vegetation indices for estimation of light conversion efficiency in
654 managed coniferous forests in Japan. *Agricultural and Forest Meteorology*, 148, 776-787.
655 Nakaji, T., Oguma, H., & Fujinuma, Y. (2006). Seasonal changes in the relationship between
656 photochemical reflectance index and photosynthetic light use efficiency of Japanese larch
657 needles. *International Journal of Remote Sensing*, 27, 493–509.
658 Nakaji, T., Oguma, H., & Hiura, T. (2011). Ground-based monitoring of the leaf phenology of
659 deciduous broad-leaved trees using high resolution NDVI camera images. *Journal of*
660 *Agricultural Meteorology*, 67, 65-74.

661 Nichol, C.J., Huemmrich, K.F., Black, T.A., Jarvis, P.G., Walthall, C.L., Grace, J., & Hall, F.G.
662 (2000). Remote sensing of photosynthetic-light-use efficiency of boreal forest. *Agricultural*
663 *and Forest Meteorology,* 101, 131–142.
664 Nichol, C.J., Lloyd, J., Shibistova, O., Arneth, A., Roser, C., Knohl, A., Matsubara, S., & Grace,
665 J. (2002). Remote sensing of photosynthetic-light-use efficiency of a Siberian boreal forest.
666 *Tellus,* 54, 677–687.
667 Ohkubo, S., Kosugi, Y., Takanashi, S., Matuo, N., Tani, M., & Abdul Rahim, N. (2008).
668 Vertical profiles and strage fluxes of CO_2, heat and water in a tropical rainforest at Pasoh,
669 Penislar Malaysia. *Tellus*, 60B, 569-582.
670 Osada, N., Takeda, H., Furukawa, A., Okuda, T. & Awang, M. (2003). Leaf phenology of trees
671 in Pasoh Forest Reserve. In: T. Okuda, K. Niiyama, S.C. Thomas, P.S. Ashton (Eds.),
672 Pasoh: Ecology of a Lowland Rain Forest in Southeast Asia (pp. 111-121). Tokyo:
673 Springer-Verlag.
674 Osada, N., Tokuchi, N. & Takeda, H. (2012). Continuous and fluctuating leaf phenology of
675 adults and seedlings of a shade-tolerant emergent tree, *Dipterocarpus sublamellatus*, in
676 Malaysia. *Biotropica*, 44, 618-626.
677 Peñuelas, J., & Filella, I. (1998). Visible and near-infrared reflectance techniques for diagnosing
678 plant physiological status. *Trends in Plant Sci*ence, 3, 151–156.
679 Peñuelas, J., Filella, I., & Gamon, J.A. (1995). Assessment of photosynthetic radiation-use
680 efficiency with spectral reflectance. *New Phytologist,* 131, 291–296.

681 Peñuelas, J., Filella, I., Biel, C., Serrano, L., & Save, R. (1993). The reflectance at the 950–970
682 nm region as an indicator of plant water status. *International Journal of Remote Sensing*,
683 14, 1887–1905.
684 Peñuelas, J., Gamon, J.A., Fredeen, A.L., Merino, J., & Field, C.B. (1994). Reflectance indexes
685 associated with physiological changes in nitrogen- and water-limited sunflower leaves.
686 *Remote Sensing of Environment,* 48, 135−146.
687 Peñuelas, J., Garbulsky, M.F., & Filella, I. (2011). Photochemical reflectance index (PRI) and
688 remote sensing of plant CO_2 uptake. *New Phytologist*, 191, 596–599.
689 Peñuelas, J., Pinol, J., Ogaya, R., & Filella, I. (1997). Estimation of plant water concentration by
690 the reflectance water index WI (R900/R970). *International Journal of Remote Sensing*, 14,
691 1887–1905.
692 Potter, C.S., Randerson, J.T., Field, C.B., Matson, P.A., Vitousek, P.M., Mooney, H.A., &
693 Klooster, S.A. (1993). Terrestrial ecosystem production: a process model based on global
694 satellite and surface data. *Global Biogeochemical Cycles*, 7, 811–841.
695 Rahimzadeh-Bajgiran, P., Munehiro, M., & Omasa, K. (2012). Relationships between the
696 photochemical reflectance index (PRI) and chlorophyll fluorescence parameters and plant
697 pigment indices at different leaf growth stages. *Photosynthesis Research*,
698 10.1007/s11120-012-9747-4.
699 Rahman, A. F., Cordova, V. D., Gamon, J. A., Schmid, H. P., & Sims, D. A. (2004). Potential
700 of MODIS ocean bands for estimating CO2 flux from terrestrial vegetation: A novel

approach. Geophysical Research Letters, doi:10.1029/ 2004GL019778, 31.

Richardson, A.D., Jenkins, J.P., Braswell, B.H., Hollinger, D.Y., Ollinger, S.V., & Smith, M.-L. (2007). Use of digital webcam images to track spring green-up in a deciduous broadleaf forest. *Oecologia* 152, 323–334.

Ruimy, A., Saugier, B., & Dedieu, G. (1994). Methodology for the estimation of terrestrial net primary production from remotely sensed data. *Journal of Geophysical Research,* 99(D3), 5263–5283.

Running, S.W., Thornton, P.E., Nemani, R.R., & Glassy, J.M. (2000). Global terrestrial gross and net primary productivity from the Earth observing system. In: O.E. Sala, R.B. Jackson, H.A. Mooney, R.W. Howarth (Eds.), Methods in Ecosystem Science (pp. 44– 57). New York: Springer-Verlag.

Serrano, L. & Peñuelas, J. (2005). Assessing forest structure and function from spectral transmittance measurements: a case study in a Mediterranean holm oak forest. *Tree Physiology,* 25, 67–74.

Sims, D.A., & Gamon, J.A. (2002). Relationships between leaf pigment content and spectral reflectance across a wide range of species, leaf structures and developmental stages. *Remote Sensing of Environment,* 81, 337–354.

Sims, D.A., Luo, H., Hastings, S., Oechel, W.C., Rahman, A.F., & Gamon, J.A. (2006). Parallel adjustments in vegetation greenness and ecosystem CO_2 exchange in response to drought in a Southern California chaparral ecosystem. *Remote Sensing of Environment,* 103, 289-303.

721 Soudani, K., Hmimina, G., Delpierre, N., Pontailler, J.-Y., Aubinet, M., Bonal, D., Caquet, B.,
722 de Grandcourt, A., Burban, B., Flechard, C., Guyon, D., Granier, A., Gross, P., Heinesh, B.,
723 Longdoz, B., Loustau, D., Moureaux, C., Ourcival, J.-M., Rambal, S., Saint André, L., &
724 Dufrêne, E. (2012). Ground-based Network of NDVI measurements for tracking temporal
725 dynamics of canopy structure and vegetation phenology in different biomes. *Remote*
726 *Sensing of Environment,* 123, 234-245.
727 Strachan, I.B., Pattey, E., & Boisvert, J.B. (2002). Impact of nitrogen and environmental
728 conditions on corn as detected by hyperspectral reflectance. *Remote Sensing of*
729 *Environment,* 80, 213–224.
730 Suárez, L., Zarco-Tejada, P.J., Berni, J.A.J., González-Dugo, V., & Fereres, E. (2009).
731 Modelling PRI for water stress detection using radiative transfer models. *Remote Sensing of*
732 *Environment,* 113, 730-744.
733 Suárez, L., Zarco-Tejada, P.J., Sepulcre-Cantó, G., Pérez-Priego, O., Miller, J.R.,
734 Jiménez-Muñoz, J.C., & Sobrino, J. (2008). Assessing canopy PRI for water stress
735 detection with diurnal airborne imagery. *Remote Sensing of Environment,* 112, 560-575.
736 Tucker, C.J. (1979). Red and photographic infrared linear combinations for monitoring
737 vegetation. *Remote Sensing of Environment,* 8, 127–150.
738 Viña, A., Gitelson, A.A., Nguy-Robertson, A.L., & Peng, Y. (2011). Comparison of different
739 vegetation indices for the remote assessment of green leaf area index of crops. *Remote*
740 *Sensing of Environment,* 115, 3468-3478.

741 Vourlitis, G.L., Priante Filho, N., Hayashi, M.M.S., Nogueira, J.De.S., Caseiro F.T., & Holanda
742 Campelo Jr., J. (2001). Seasonal variations in the net ecosystem CO2 exchange of a mature
743 Amazonian transitional tropical forest (cerradão). *Functional Ecol*ogy, 15, 388-395.
744 White, M.A., Thornton, P.E., & Running, S.W. (1997). A continental phenology model for
745 monitoring vegetation responses to interannual climatic variability. *Global Biogeochemical*
746 *Cycles*, 11, 217-234.
747 Wu, C., Niu, Z., Tang, Q., Huang, W., Rivard, B., & Feng, J. (2009). Remote estimation of gross
748 primary production in wheat using chlorophyll-related vegetation indices. *Agricultural and*
749 *Forest Meteorology*, 149, 1015−1021.
750 Zarco-Tejada, P.J., González-Dugo, V., & Berni, J.A.J. (2012). Fluorescence, temperature and
751 narrow-band indices acquired from a UAV platform for water stress detection using a
752 micro-hyperspectral imager and a thermal camera. *Remote Sensing of Environment*, 117,
753 322-337.
754
755 **Figure legends**
756
757 **Fig. 1.** Typical spectra of (a) irradiance, reflected radiance and correction factor, and (b) the
758 spectral features of canopy reflectance and derived reflectance. The wavelengths used for
759 the five VIs are also shown.
760

761 **Fig. 2.** Canopy photo of dipterocarp trees near the monitoring tower. The canopies of monitored
762 trees (*Dipterocarpus sublamellatus* #1 and #2) are outlined in red (a). The four photos show
763 representative foliar phenological stages of *D. sublamellatus* #1 observed in the first half of
764 2010. Before the leaf flush, dark green leaves covered the canopy top (a). The new leaf
765 emergence was observed from April 2, together with defoliation, and new orange-coloured
766 leaves appeared on over half of the canopy on 16 April (b). Defoliation was almost
767 complete within ~1 month (c), but new leaf flush and leaf expansion continued over 3
768 months (d). In this study, the timing of leaf flush was defined as the date when new leaf
769 flush was observed over half the area of the canopy.
770
771 **Fig. 3.** Relationship of solar zenith angle and (a–e) VIs and (f) solar radiation during a year. The
772 half-hourly data from 9 to 16 h in 2009 are shown. Red-coloured square indicates the data
773 range used for correlation analysis in this paper.
774
775 **Fig. 4.** Time courses of air temperature (T_{air}), vapor pressure deficit (VPD) and volumetric soil
776 water content (SWC) at the lowland dipterocarp forest in Pasoh Forest Reserve, from
777 October 2008 to December 2011 (a). Fraction of absorbed photosynthetically active
778 radiation (FAPAR) and absorbed photosynthetically active radiation (APAR) are shown in
779 the lower part of (b).
780

781 **Fig. 5.** Time courses of productivity parameters (a) and spectral vegetation indices (b, c) at the
782 lowland dipterocarp forest in the Pasoh Forest Reserve. Each dot indicates the mean value
783 around the culmination period (12:00–14:00). The solid lines are 7-day moving average
784 values. The seven arrows and dotted red lines indicate the timing of new leaf flush of
785 *Dipterocarpus sublamellatus* trees monitored from September 2009. The data gaps from
786 November 2010 to February 2011 were caused mainly by instrumental error due to
787 thunderstorm activity.
788
789 **Fig. 6.** Accuracy of the empirical regression models. The data of four test cases showing the
790 highest R^2 value within each regression group are analyzed. Each dot is the mean value
791 around the culmination time (12:00–14:00). The dashed line indicates the 1:1 line. The
792 relative root mean square error (*r*RMSE) was calculated for the predicted LUE using a
793 resubstitution estimate.

Table 1

Table 1. List of the vegetation indices (VIs) calculated using the tower-monitored spectral reflectances. ρ_λ and d_λ indicate reflectance value and first derivative of reflectance at wavelength of λ nm. Some wavelengths in the original VIs were changed to the wavebands of the spectroradiometers used.

VI	Formulation	General target(s)	Reference
NDVI	$(\rho_{857}-\rho_{647})/(\rho_{857}+\rho_{647})$	FAPAR, LAI, greenness	Tucker (1979), Gamon et al. (1995)
EVI	$((\rho_{857}-\rho_{647})/(1+\rho_{857}+6\rho_{647}-7.5\rho_{466}))\times 2.5$	FAPAR, GPP, greenness	Liu and Huete (1995), Huete et al. (2002)
WI	ρ_{900}/ρ_{970}	Plant water status	Peñuelas et al. (1993, 1997)
PRI	$(\rho_{531}-\rho_{570})/(\rho_{531}+\rho_{570})$	LUE, carotenoid/chlorophyll ratio	Gamon et al. (1992, 1997), Peñuelas et al. (1995)
CCI	d_{720}/d_{700}	Chlorophyll content	Sims et al. (2006)

Table 2

Table 2. Regression analysis for the estimation of LUE using meteorological parameters and/or spectral vegetation indices (n = 699). The variable(s) showing the highest coefficient of determination in each regression group is shown in bold.

Model	Variable	R^2	P	Function
Single regression	**PRI**	0.116	< 0.001	LUE = 0.256 PRI + 0.023 [a]
(VI)	CCI	0.081	< 0.001	LUE = 0.017 CCI – 0.014
	EVI	0.043	< 0.001	LUE = 0.057 EVI – 0.009
	WI	0.046	< 0.001	LUE = – 0.075 WI + 0.088
	NDVI	0.011	< 0.01	LUE = – 0.028 NDVI + 0.038
(meteorological factor)	**VPD**	0.336	< 0.001	LUE = – 0.00074 VPD + 0.025
	Tair	0.201	< 0.001	LUE = – 0.0016 Tair + 0.061
	SWC	0.110	< 0.001	LUE = 0.041 SWC – 0.001
(combination)	**PRI*VPD**	0.352	< 0.001	LUE = 0.0174 (PRI*VPD) + 0.023 [b]
	PRI*Tair	0.190	< 0.001	LUE = 0.0109 (PRI*Tair) + 0.025
Multiple regression	**PRI, VPD**	0.375	< 0.001	LUE = 0.153 PRI – 0.00067 VPD + 0.029
(2 variables)	PRI, Tair	0.309	< 0.001	LUE = 0.244 PRI – 0.0015 Tair + 0.067

The combination of VPD, PRI and EVI was selected as the best explanatory variables in the stepwise multiple regression analysis when using three variables and with the threshold VIF < 2.0.

[a] This relationship can also be expressed in the form of an exponential function, as LUE = 0.0249 $e^{16.20\text{PRI}}$ (r^2 = 0.126).

[b] If the LUE_{max} is defined as the maximum value of weekly mean LUE (0.022 mol mol^{-1}), the regression function is denoted as follows: LUE = LUE_{max} (1.02 + 0.79 (PRI*VPD)).

Figure 1

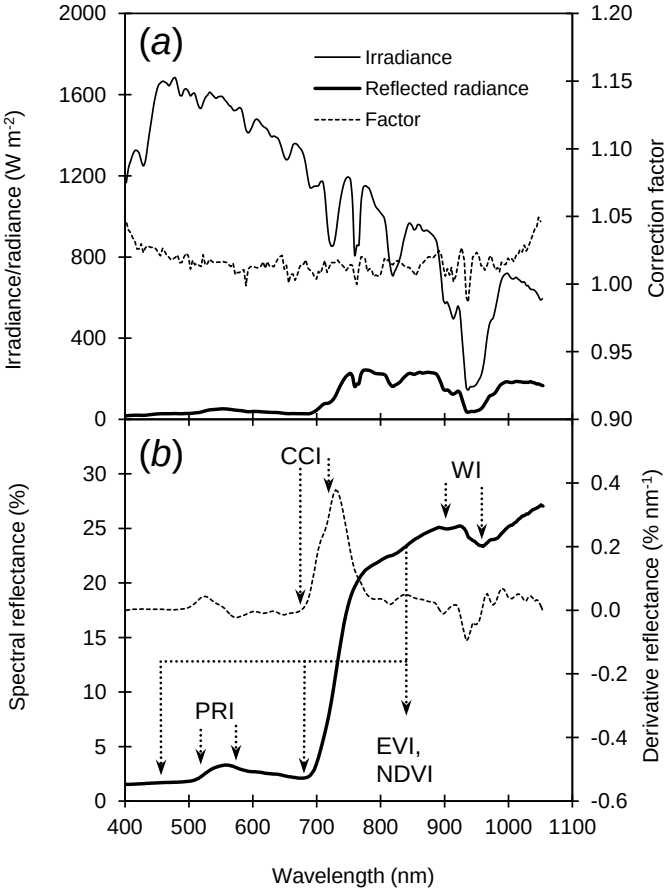
(a)
Irradiance
Reflected radiance
Factor
Irradiance/radiance (W m-2)
Correction factor
2000
1600
1200
800
400
0
1.20
1.15
1.10
1.05
1.00
0.95
0.90
(b)
CCI
WI
PRI
EVI,
NDVI
Spectral reflectance (%)
Derivative reflectance (% nm-1)
30
25
20
15
10
5
0
0.4
0.2
0.0
-0.2
-0.4
-0.6
400
500
600
700
800
900
1000
1100
Wavelength (nm)

Figure 2

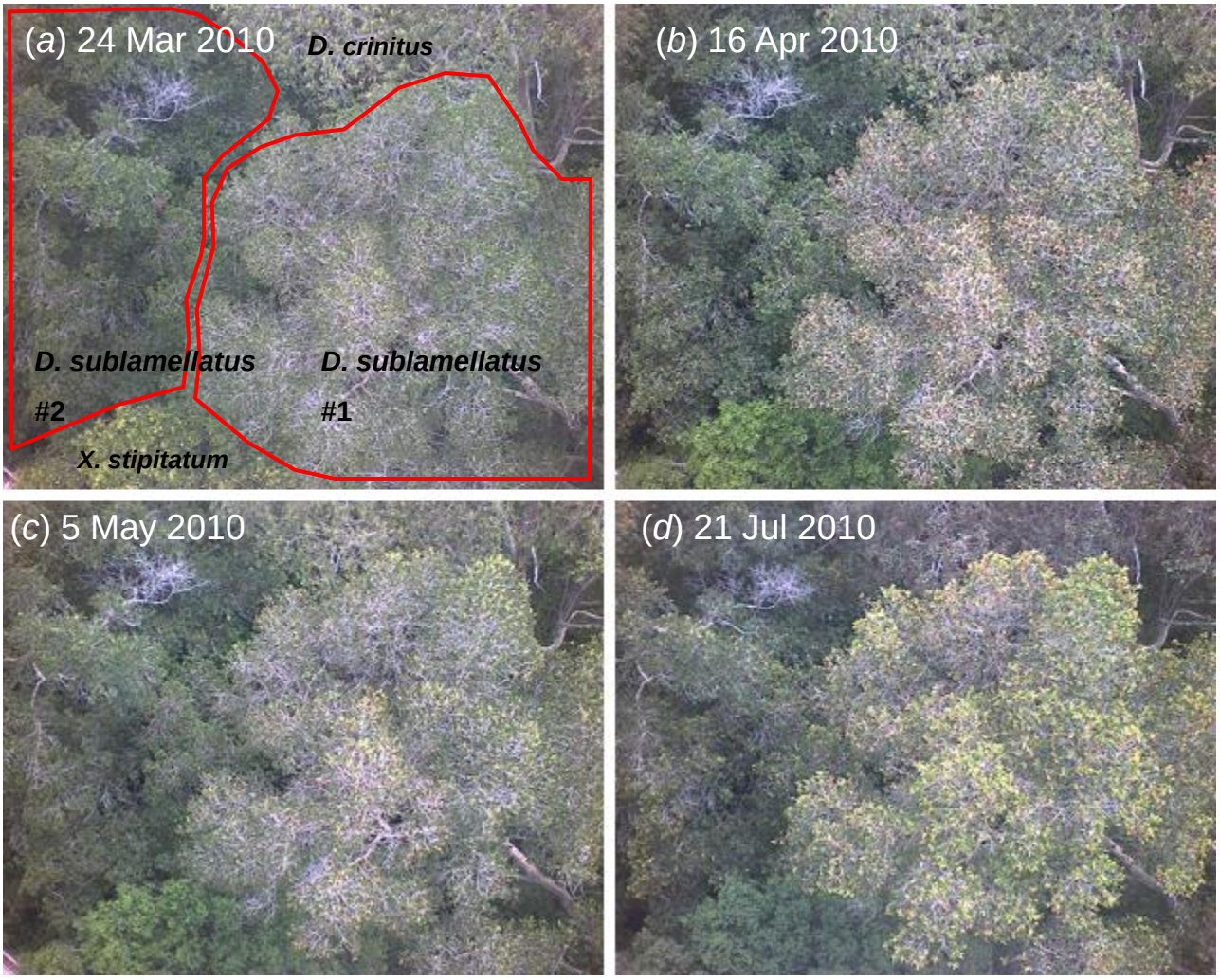
(a) 24 Mar 2010
D. crinitus
D. sublamellatus #2
D. sublamellatus #1
X. stipitatum
(b) 16 Apr 2010
(c) 5 May 2010
(d) 21 Jul 2010

Figure 3

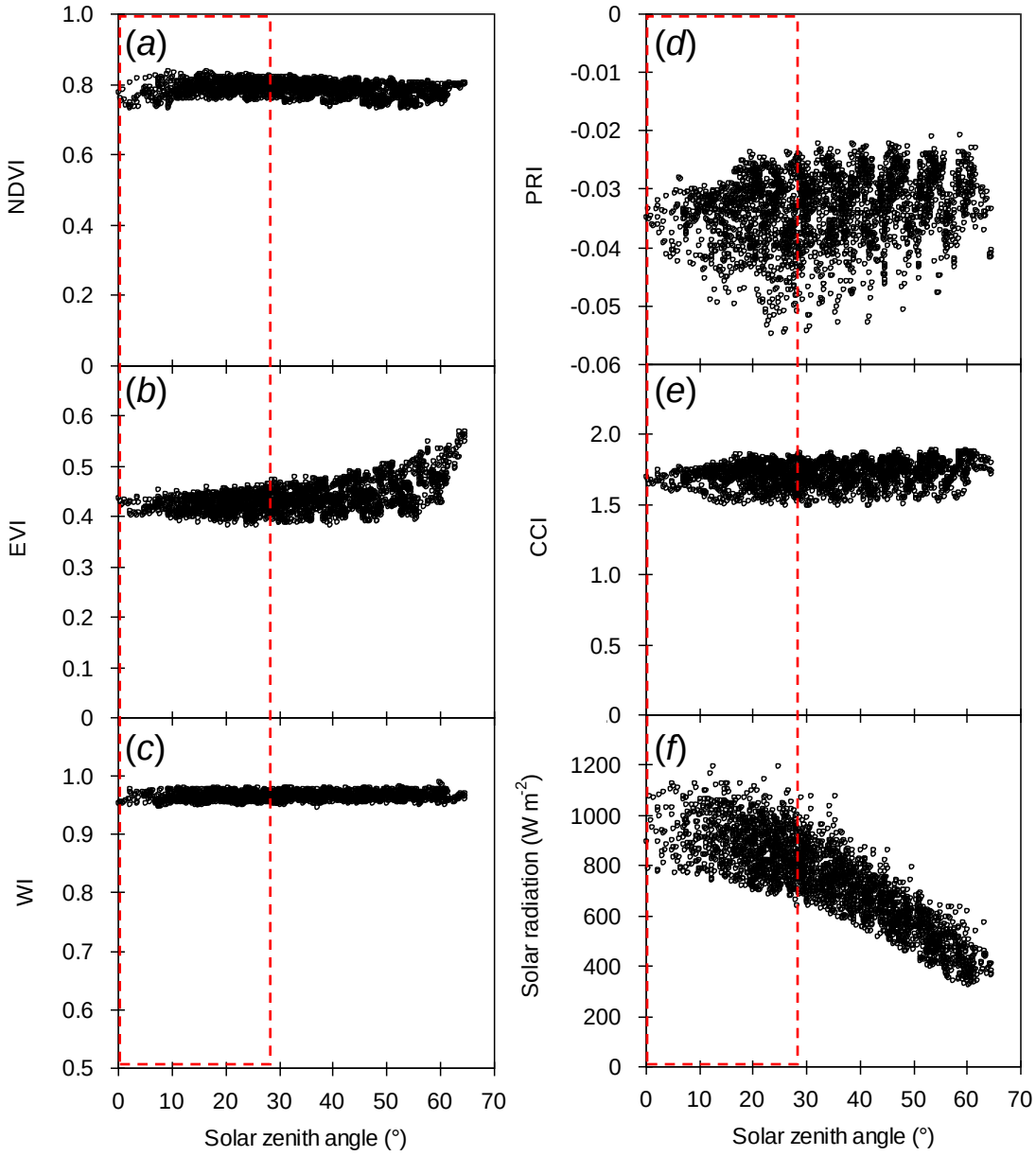
(a)
(b)
(c)
(d)
(e)
(f)
NDVI
EVI
WI
PRI
CCI
Solar radiation (W m-2)
Solar zenith angle (°)
Solar zenith angle (°)

Figure 4

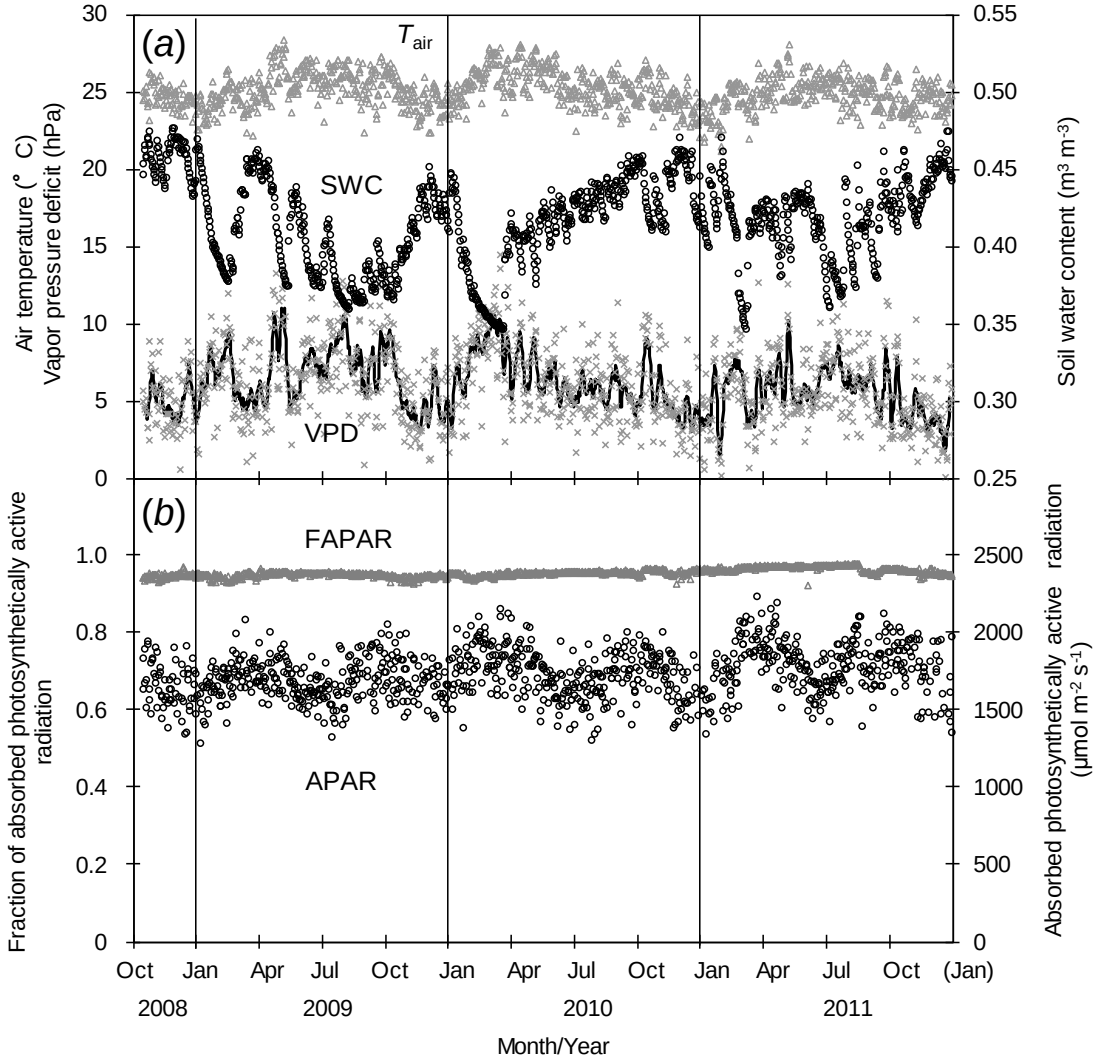
(a)
T_{air}
SWC
VPD
Air temperature (° C)
Vapor pressure deficit (hPa)
Soil water content (m³ m⁻³)
(b)
FAPAR
APAR
Fraction of absorbed photosynthetically active radiation
Absorbed photosynthetically active radiation (µmol m⁻² s⁻¹)
Oct Jan Apr Jul Oct Jan Apr Jul Oct Jan Apr Jul Oct (Jan)
2008 2009 2010 2011
Month/Year

Figure 5

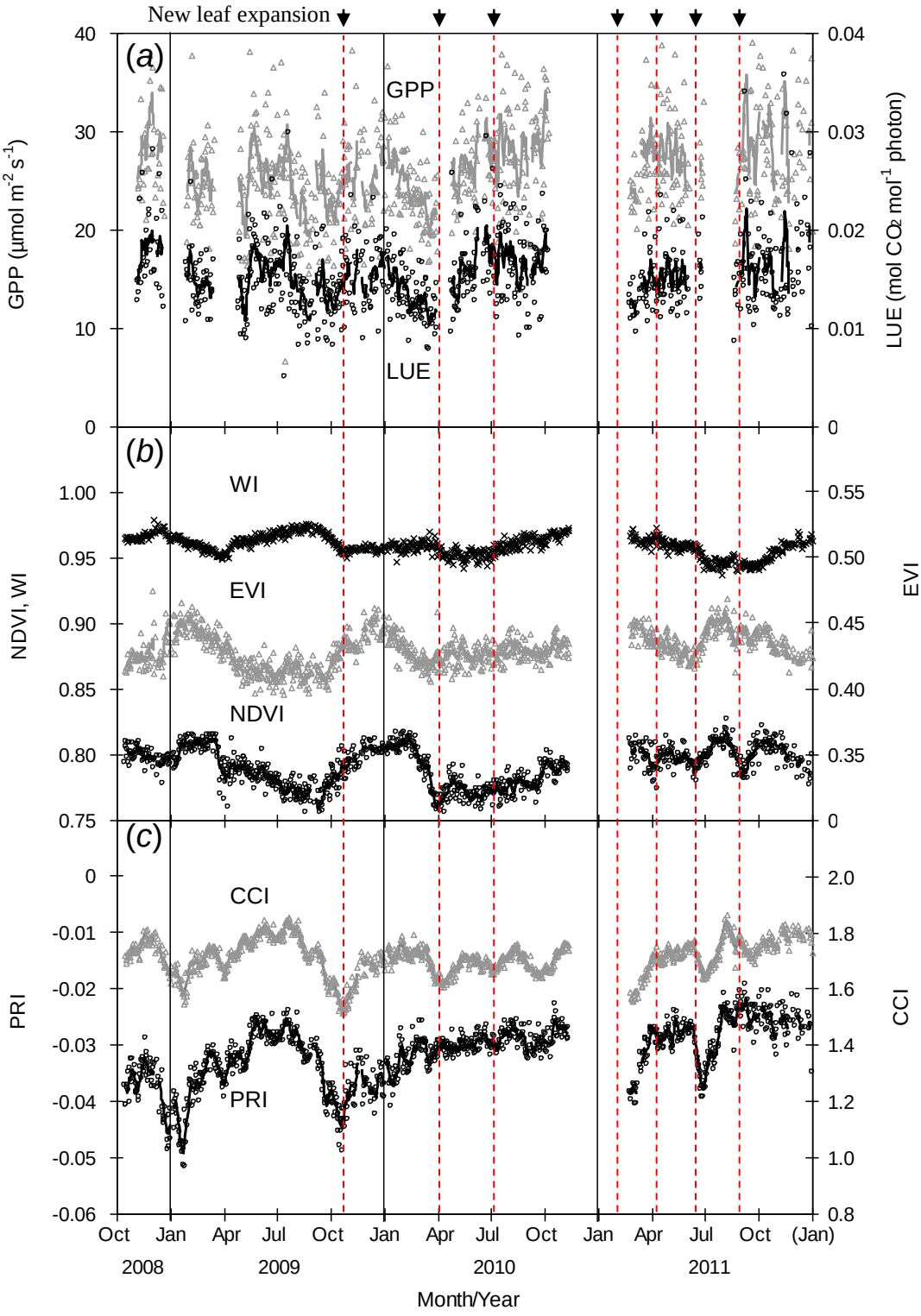
New leaf expansion
(a)
GPP
LUE
GPP (µmol m-2 s-1)
LUE (mol CO2 mol-1 photon)
(b)
WI
EVI
NDVI
NDVI, WI
EVI
(c)
CCI
PRI
PRI
CCI
Oct
Jan
Apr
Jul
Oct
Jan
Apr
Jul
Oct
Jan
Apr
Jul
Oct
(Jan)
2008
2009
2010
2011
Month/Year

Figure 6

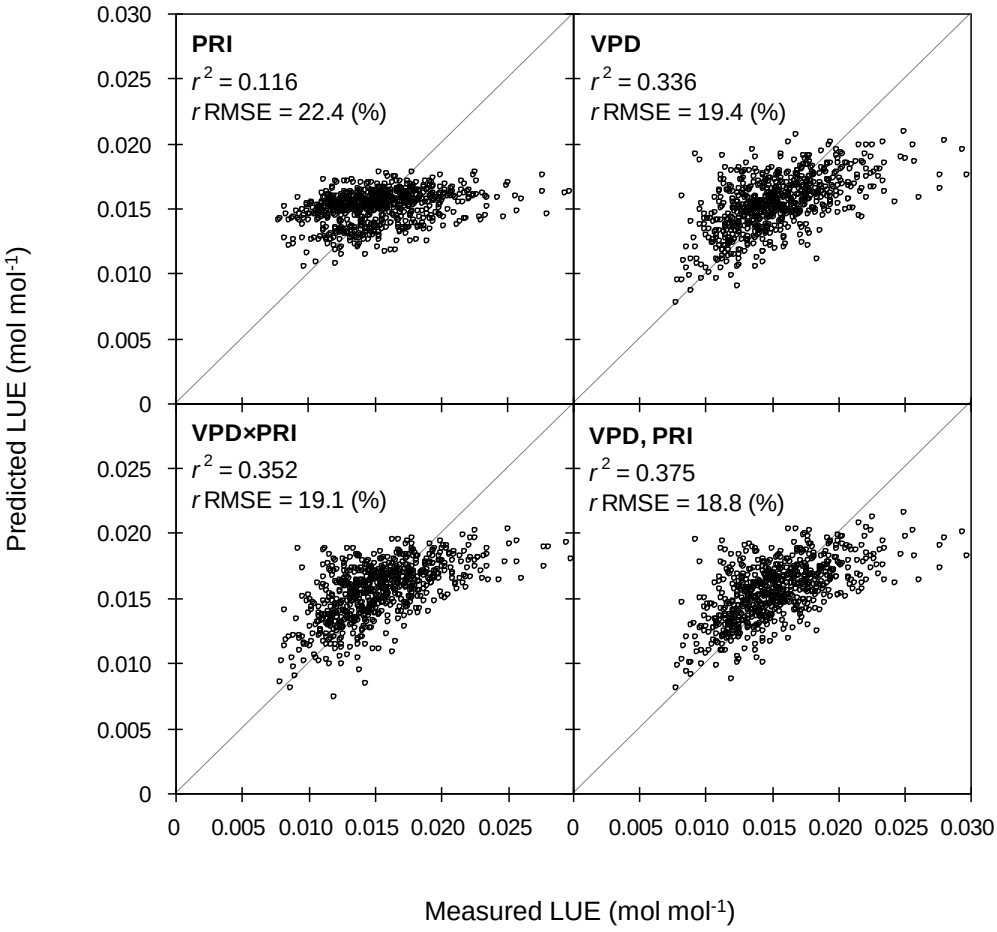
PRI
r^2 = 0.116
r RMSE = 22.4 (%)
VPD
r^2 = 0.336
r RMSE = 19.4 (%)
VPD×PRI
r^2 = 0.352
r RMSE = 19.1 (%)
VPD, PRI
r^2 = 0.375
r RMSE = 18.8 (%)
Predicted LUE (mol mol-1)
Measured LUE (mol mol-1)
0
0.005
0.010
0.015
0.020
0.025
0.030